On the Accuracy of Split-Step Fourier Simulations for Wideband Nonlinear Optical Communications

Simone Musetti, Paolo Serena, *Member, IEEE*, and Alberto Bononi, *Senior Member, IEEE*

***Abstract*—We investigate the accuracy of wideband split-step Fourier method (SSFM) simulations by treating SSFM numerical noise as an additive distributed noise source, much like amplified spontaneous emission and nonlinear interference. In this framework, we emphasize that the step size of a numerical simulation targeting a given error on the received signal-to-noise ratio (SNR) should be launch-power independent, and should scale inversely with the square of the signal bandwidth. From this we conclude that the commonly used nonlinear phase criterion for the step update along the distance is not optimal due to its power dependence and its unawareness of signal bandwidth. We propose a general criterion, based on four-wave mixing control, to set the first step of a series of exponentially increasing steps at the desired received SNR accuracy. Finally, we discuss the behavior of the SSFM accuracy versus step-size showing that at practical accuracies of interest the well-known arguments based on the Baker–Campbell–Hausdorff formula may not hold, and explain how to set up a correct SSFM simulation to target an acceptable SNR error.**

***Index Terms*—Nonlinear phase criterion, numerical simulation, split-step fourier method.**

I. Introduction

SINCE a closed form solution of the nonlinear Schrödinger equation (NLSE) does not exist in the general case, numerical algorithms are necessary to estimate the evolution of the electric field along an optical fiber. Among the algorithms available in the literature, the split-step Fourier method (SSFM) is the most widely used for its simplicity and efficiency [1]. The SSFM discretizes the propagation distance in small steps, and approximates the propagation within each step by the concatenation of elementary operations for which a closed form solution is available. The elementary operations are usually identified in the linear/nonlinear effects of the NLSE.

Such a split-step technique unavoidably introduces numerical errors. However, since SSFM is a convergent method, the numerical error can be mitigated by shortening the steps at the expense of simulation complexity. The complexity is generally dominated by the operations performed both in fast Fourier transforms (FFT) and in the numerical computations of exponential functions of the linear and nonlinear operators. Optimizing the number and the implementation of such operations is thus extremely important to reduce the computational effort for a given accuracy.

The first attempt to improve SSFM was to adopt the symmetric splitting technique for the step size, where nonlinearity is sandwiched between two half-length linear steps. In numerical analysis, such a rule is also referred to as the Strang splitting scheme [2]. Although this choice increases the number of operations per step, on a global scale after concatenating many steps the scheme appears identical to the classical asymmetric step selection rule except for the first/last step, hence at a minor additional cost [3]. The symmetric split-step is generally proposed as a better option than the asymmetric split-step because of a higher order local accuracy, i.e., the local error approaches zero at least cubically in the step length instead of quadratically as for the asymmetric split-step. On these grounds, other more complex methods to increase the order of accuracy with the step length have been proposed [4], [5].

Most of the investigations in optimizing SSFM have been focused on variable step-size selection rules [3], [4], [6]–[8]. Bosco *et al.* [6] proposed a logarithmic variable step-size in order to efficiently suppress the numerical four-wave mixing (FWM) enhancement typically arising in constant step discretization of the fiber [9]. Sinkin *et al.* [4] proposed an adaptive step-size method based on estimating and bounding the local error along propagation. Another popular method is the nonlinear phase criterion [4], which bounds the maximum amount of nonlinear phase shift in the step. Zhang *et al.* proposed a variable step-size rule targeting a given global error [7], [8]. The key point of this method is to increase the step length on the basis of the scaling properties of the local error per step with system parameters, such as fiber dispersion, attenuation, and signal bandwidth.

All these studies focused on the relative error introduced by SSFM, i.e., the numerical error variance normalized to the signal power. Therefore they concentrate on the accuracy of the electric field calculation without considering its implications for signal detection. However, the simulation of modern communication systems based on coherent detection usually targets an estimate of the system performance such as the signal-to-noise ratio (SNR) after matched filter detection. In this framework, a reliable numerical SSFM should bound the error on the SNR. From this novel perspective, the numerical error variance should be compared to the variance of the amplified spontaneous emission (ASE) and the nonlinear interference (NLI) introduced by the optical link rather than to the signal power. In this paper, we

Manuscript received July 10, 2018; revised September 17, 2018; accepted October 18, 2018. Date of publication October 22, 2018; date of current version November 21, 2018. This work was supported by Nokia Bell-labs, Villarceaux, France. *(Corresponding author: Simone Musetti.)*

The authors are with the Department of Ingegneria e Architettura, Università di Parma, Parma 43124, Italy (e-mail: simone.musetti@studenti.unipr.it; paolo.serena@unipr.it; alberto.bononi@unipr.it).

Color versions of one or more of the figures in this paper are available online at http://ieeexplore.ieee.org.

Digital Object Identifier 10.1109/JLT.2018.2877384

will show the implications that such a different point of view has on the setup of a numerical SSFM simulation.

So far the computing resources available to simulate optical propagations have been more than adequate, thus a fine calibration of SSFM accuracy did not capture much attention. However, the situation is drastically changing in the near future since bandwidth-hungry Internet applications are pushing the research into studying the occupation of the whole optical C-band and beyond [10], [11]. In this new scenario, the computational effort of trustable SSFM simulations will skyrocket, resulting in extensive time-consuming simulations even with the help of graphics processing units (GPUs). A simple argument to understand this claim is the following. For a reliable SSFM, the step size should be comparable with the characteristic lengths of the NLSE. Of particular interest is the dispersion length which expresses the distance over which linear effects induce significant changes on the electric field. Since the dispersion length scales with the square of the bandwidth, it rapidly gets very small in a wide bandwidth scenario, thus calling for huge computational efforts. How the accuracy of the simulation is affected is also yet to be precisely defined. It is therefore important to minimize the computational effort of SSFM while being sure to maintain an acceptable accuracy.

This paper, which is an extension of [12] in terms of both novel theoretical and numerical results, aims at finding general scaling rules of the SSFM accuracy and providing simple guidelines on how to set up an efficient yet accurate SSFM simulation. We propose a different framework for the SSFM error analysis, which is more natural to the system designer that normally expresses the performance in terms of the received SNR. We show that a given error in decibels (dB) on the SNR is independent of signal power, hence that there is no need to shorten the steps at increasing power, as in popular adaptive step size methods [4], [6]–[8]. Moreover, we discuss the reason of the SSFM accuracy by showing that the global second/first order accuracy of the symmetric/asymmetric split-step [4], [5], [8], respectively, holds only at unrealistically high precisions. At practical precisions, the advantage of the symmetric split-step is much more limited compared to the asymmetric split-step.

In our simulations, we push the signal bandwidth up to 5 THz so as to cover the whole C-band of Erbium-doped fiber amplifiers (EDFA).

The paper is organized as follows: in Section II we analyze the SSFM error in the framework of the SNR. In particular, we propose a new parameter to set SSFM simulations at the desired SNR error. In Section III we report the main results on SSFM accuracy arising from such an approach. In Section V we perform a computational analysis of the SSFM and compare two popular step-size updating rules in terms of computational effort. Finally, we draw our main conclusions.

II. SSFM Error Analysis

The accuracy of a simulation should be referred to the target parameter on which performance is evaluated. In coherent optical communications, the performance is typically expressed in terms of the SNR. The SNR can be usually directly converted to bit error rate (BER), for instance under the assumption of additive Gaussian noise. In this framework, the accuracy of the simulation is therefore the accuracy in the SNR estimation. Moreover, since the SNR is generally expressed in decibels, a reliable SSFM simulation should be such that the SNR is estimated with a bounded accuracy error in dB, as sketched in Fig. 1 by the constant error bars. The dashed line indicates the SNR considering just the numerical error of the simulation, that should have a fixed gap in a dB scale from the "true" SNR in order to have a fixed accuracy. We proceed now to analyze the numerical error under this novel point of view.

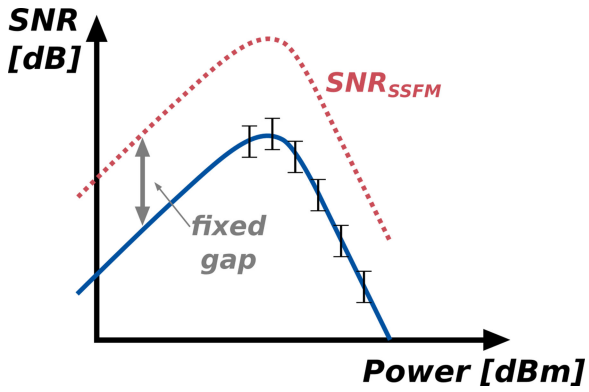

Fig. 1. Visual representation of an ideal simulation setup. The error bars on the estimated SNR curve should remain constant whatever the transmitted signal power. The dashed curve ($\mathrm{SNR}_{\mathrm{SSFM}}$) represents the SNR due only to the numerical error, that should have a fixed gap from the estimated SNR curve.

A. Perturbative Analysis of SSFM Error

The propagation equation within an optical fiber is well described by the Manakov equation [13], [14], which provides reliable estimations even over large bandwidths [15]. At coordinate z and time t the Manakov equation in operator notation is:

$$\frac{\partial A\left(z,t\right)}{\partial z}=\left(\mathcal{L}+\mathcal{N}\right)A \tag{1}$$

where $A\left(z,t\right)=\left[A_x,\,A_y\right]$ is the optical signal with A_x and A_y the polarization tributaries, and the linear and nonlinear operators are defined respectively as:

$$\begin{aligned}\mathcal{L} &\triangleq j\frac{\beta_2}{2}\frac{\partial^2}{\partial t^2}\\ \mathcal{N}A\equiv\mathcal{N}\left(A\right) &\triangleq -j\frac{8}{9}\gamma e^{-\alpha z}\left(A^{\dagger}A\right)A\end{aligned} \tag{2}$$

where β_2, α, γ are respectively the chromatic dispersion, attenuation and nonlinear coefficient of the optical fiber, while $\dagger$ means transpose-conjugate. With the change of variable $A\left(z,t\right)\triangleq e^{\mathcal{L}z}U\left(z,t\right)$ we can express the NLSE in integral form (see Appendix A):

$$U\left(z,t\right)=U\left(0,t\right)+\int_0^z e^{-\mathcal{L}\xi}\mathcal{N}\left(e^{\mathcal{L}\xi}U\left(\xi,t\right)\right)\mathrm{d}\xi \tag{3}$$

where $U\left(z,t\right)$ is the optical field in a reference system that tracks all the linear effects.

There is no general closed-form solution to (3). Two popular approximated methods properly fix the propagation coordinate ξ within either $U(\xi,t)$ or $e^{\mathcal{L}\xi}$ to simplify the problem. For instance, if we force $U(\xi,t) \equiv U(0,t)$ at any coordinate and let $e^{\mathcal{L}\xi}$ free to vary with ξ, we can close the integral in (3) obtaining the first-order regular perturbation (RP1), i.e., the first-order Volterra solution of the NLSE [16]. In this framework, the variations of $e^{\mathcal{L}\xi}$ along ξ are analytically integrated for any $\mathcal{L}$, but unfortunately they are applied to the transmitted signal whatever the coordinate. This assumption is reliable only if nonlinearity induces a small perturbation on U from 0 to z.

On the other side, we can concentrate linear effects at a given coordinate $0 \leq \xi_0 \leq z$ and let the approximated solution $\widehat{U}(\xi,t)$ free to vary along ξ:

$$\widehat{U}\,(z,t) = U\,(0,t) + e^{-\mathcal{L}\xi_0} \int_0^z \mathcal{N}\left(e^{\mathcal{L}\xi_0}\,\widehat{U}\,(\xi,t)\right) \mathrm{d}\xi\,. \tag{4}$$

We can still integrate exactly (4) obtaining the SSFM solution, as shown in Appendix A. In particular, if $\xi_0 = 0$ we get the asymmetric SSFM, while if $\xi_0 = \frac{z}{2}$ we get the symmetric SSFM. In this framework, SSFM is thus reliable when linear effects induce small perturbations on U from 0 to z. The differences between RP1 and SSFM are similar to the differences between the Filon's and the Gaussian quadrature methods for numerical integration of functions [17].

Both RP1 and SSFM approximate the integral in (3). The SSFM error $e_{\text{SSFM}} \triangleq U\,(z,t) - \widehat{U}\,(z,t)$ appears as an additive perturbation as much as the nonlinear interference (NLI) induced by the Kerr effect on the signal. Hence, under perturbative assumptions [18]–[21], we may modify the received SNR as:

$$\widehat{\text{SNR}} = \frac{P}{\sigma^2_{\text{ASE}} + \sigma^2_{\text{NLI}} + \sigma^2_{\text{SSFM}}} \tag{5}$$

where P is the signal power while σ^2_{ASE}, σ^2_{NLI} and σ^2_{SSFM} are the variance of amplified spontaneous emission (ASE) noise, nonlinear interference and SSFM error e_{SSFM}, respectively, all assumed mutually uncorrelated for simplicity. In the following we will refer to $\text{SNR} \triangleq \widehat{\text{SNR}}(\sigma^2_{\text{SSFM}} = 0)$ as the *true*, unknown, SNR. A first consequence of (5) is that the estimation $\widehat{\text{SNR}}$ is always smaller than SNR for any link, under the uncorrelation assumption.

The relative SNR error due to SSFM can be defined as:

$$\frac{\text{SNR}}{\widehat{\text{SNR}}} \triangleq 1 + \frac{\sigma^2_{\text{SSFM}}}{\sigma^2_{\text{NLI}} + \sigma^2_{\text{ASE}}}.$$

Since all variances are positive, the relative SNR error is a monotonically decreasing function of σ^2_{ASE}, hence in dB the error is bounded by:

$$0 \leq \left(\frac{\text{SNR}}{\widehat{\text{SNR}}}\right)_{\text{dB}} \leq \left(1 + \frac{\sigma^2_{\text{SSFM}}}{\sigma^2_{\text{NLI}}}\right)_{\text{dB}}. \tag{6}$$

Values of the ratio $\left(\frac{\text{SNR}}{\widehat{\text{SNR}}}\right)_{\text{dB}}$ closer to zero indicate accurate simulations. In the following we will focus on the upper bound of the SNR error as a worst case target.

Since nonlinearity $\mathcal{N}$ in (1) scales as $P\sqrt{P}$, it is convenient to factor out P^3 and define

$$a_{\text{NL}} \triangleq \sigma^2_{\text{NLI}}/P^3, \quad a_{\text{SSFM}} \triangleq \sigma^2_{\text{SSFM}}/P^3\,. \tag{7}$$

By the same arguments that show a_{NL} to be almost power independent at small NLI [21], even a_{SSFM} is reasonably power-independent at small numerical errors. As a consequence, a trustable SSFM simulation should target a fixed $a_{\text{SSFM}}/a_{\text{NL}}$ to bound a given error in dB on the SNR independently of the signal power. This criterion is not followed by popular step-size choices as we will discuss in the next section.

B. Step-Updating Rule and First Step Selection

The SSFM solution consists of discretizing the integral in (4) as a concatenation of steps. Given a certain number of steps N, a way to effectively improve the accuracy without affecting the computational effort is to use variable step-size along the distance [6]. Different variable step-size updating rules exist in the literature [3], [4], [6]–[8]. The most widely used is the nonlinear phase criterion (NLP) [4], which sets the kth step length h_k based on the maximum tolerable nonlinear phase $\Delta\phi$ accumulated in the step. The value of $h_k,\ k = 1,\ldots,N$, can be inferred by solving the implicit equation:

$$\Delta\phi \triangleq \gamma P_k L_{\text{eff}}\,(h_k) \tag{8}$$

with γ the nonlinear coefficient of the fiber, P_k the signal peak power at step input and $L_{\text{eff}}\,(h_k) \triangleq (1 - e^{-\alpha h_k})/\alpha$ the step effective length, with α the power attenuation. The rationale behind the NLP is that the error is expected to be proportional to the strength of the nonlinearity. Since nonlinearity manifests locally as self-phase modulation (SPM), such a strength can be expressed by the maximum SPM phase $\Delta\phi$. By matching $\Delta\phi$ of two consecutive steps the updating rule can be expressed as:

$$L_{\text{eff}}\,(h_{k+1}) = L_{\text{eff}}\,(h_k)\,\frac{P_k}{P_{k+1}} \simeq L_{\text{eff}}\,(h_k)\,e^{\alpha h_k} \tag{9}$$

where the last approximation ignores the peak power fluctuations due to chromatic dispersion, thus yielding a step updating rule coinciding with the logarithmic step-size rule [6]. Since power decreases along the distance because of attenuation, such a criterion stretches the step along propagation, thus reducing the computation time.

Another method proposed by Zhang *et al.* scales the step along the distance in order to keep a constant local error (CLE) [7], [8]. This yields the following step updating rule:

$$h_{k+1} = h_k \left(\frac{P_k}{P_{k+1}}\right)^{\frac{1}{q}} \simeq h_k e^{\frac{\alpha}{q} h_k} \tag{10}$$

with $q = 2$ or 3 depending of the SSFM step type, i.e., asymmetric or symmetric, respectively.

Note that all such step updating rules are iterative along the distance, hence a starting value h_1 must be chosen. The idea is that once the starting value has been set with a certain criterion, the simulation error is kept under control by the step-updating rule. The first step for the NLP can be inferred from (8) by

forcing a maximum value to $\Delta\phi$, obtaining:

$$h_1 = \begin{cases} \dfrac{1}{\alpha}\log\left(\dfrac{\gamma P_1}{\gamma P_1 - \alpha\Delta\phi}\right) & \gamma P_1 > \alpha\Delta\phi \\ L & \text{else} \end{cases} \tag{11}$$

with L the fiber length. For the CLE the following expression for the first step can be inferred from the scaling laws of the local error with system parameters [7], [8]:

$$h_1 = \frac{\Psi_{\mathrm{G}}}{(\gamma P_1)^{\frac{1}{q-1}} |\beta_2| B_{\mathrm{WDM}}^2} \tag{12}$$

with B_{WDM} the WDM signal bandwidth and Ψ_{G} a constant depending on the target global error.

Please note that P_1 is the peak power of the WDM signal, hence it is a function of B_{WDM}. For instance, in a WDM comb of evenly spaced channels with equal power, P_1 scales almost linearly with B_{WDM}.

It has been shown in [6], [9] that the numerical error of constant-step size SSFM simulations is mainly given by an over-estimation of FWM fluctuations along a step. The FWM is best described in frequency domain, where eq. (3) at frequency f reads as:

$$\tilde{U}(z,f) = \tilde{U}(0,f) - j\frac{8}{9}\gamma\int_0^z \iint_{-\infty}^{\infty} e^{-\alpha\xi} e^{j\Delta\beta\xi}\tilde{U}(\xi, f+f_1) \times \left[\tilde{U}^{\dagger}(\xi, f+f_1+f_2)\tilde{U}(\xi, f+f_2)\right] \mathrm{d}f_1 \mathrm{d}f_2 \mathrm{d}\xi\,.$$

The tilde indicates Fourier transform, while FWM is locally weighted by the function $e^{-\alpha\xi}e^{j\Delta\beta\xi}$, with $\Delta\beta \triangleq (2\pi)^2\,\beta_2\,(f-f_1)\,(f-f_2)$ the phase matching coefficient[1] [1], [6], [9]. SSFM indeed substitutes $e^{j\Delta\beta\xi}$, hence the oscillating function $e^{\mathcal{L}\xi}$ in (3), with a ξ-independent operator within each step. Nonlinearities are thus integrated over a "virtual zero-dispersion fiber" for such a step length, thus over-estimating the local FWM accumulation.

In this paper we propose to set h_1 to limit the maximum variation of $\Delta\beta\xi$. Since the worst case first-order FWM occurs for frequencies spaced apart by the signal bandwidth B_{WDM}, a FWM-aware first step h_1 can be set as:

$$h_1 = \frac{\Phi_{\mathrm{FWM}}}{|\beta_2|\,(2\pi B_{\mathrm{WDM}})^2}\,, \tag{13}$$

where Φ_{FWM} is the maximum tolerable FWM phase shift set by the user. Such a choice is power independent, thus it does not affect the accuracy at variable launch power, in agreement with our discussion in Section II-A. It is worth noting that (13) scales with B_{WDM} differently of (12) because of the above-mentioned dependence of P_1 on B_{WDM}. All the remaining steps can be set by using the step updating rule of choice. From now on we will refer to the NLP and CLE triggered with our FWM-aware criterion by FWM-NLP and FWM-CLE, respectively.

Each step-updating rule calls for a different value of Φ_{FWM} for a given accuracy. In Section IV-B (see Fig. 5) we will show by numerical simulations that a reasonable and almost universal value for Φ_{FWM} is 20 rad for the FWM-CLE and 4 rad for the FWM-NLP.

[1]Such a $\Delta\beta$ neglects third-order dispersion, which may be of concern at very low values of β_2. However, it is worth noting that SSFM for $\beta_{2,3} = 0$ yields the exact solution.

III. Simulations Setup

We investigated the accuracy of the SSFM in a wide range of scenarios. The tested signal was composed of a wavelength division multiplexing (WDM) comb of polarization division multiplexing (PDM) 16 quadrature amplitude modulation (QAM) channels spaced by $\Delta f = 50$ GHz. Each channel had symbol rate $R = 49$ GBaud, with root-raised cosine supporting pulses with roll-off 0.01. The number of channels was varied between 1 and 101 to check the SSFM accuracy at different WDM bandwidths. We thus reached a maximum simulated bandwidth of $B = 5.05$ THz, i.e., about the whole C-band. The optical link was composed of 20 spans, each of length $L = 100$ km, attenuation $\alpha = 0.2$ dB/km, nonlinear coefficient $\gamma = 1.3$ 1/W/km and zero polarization mode dispersion. The fiber dispersion was varied between 2.125 and 17 ps/nm/km with a third order dispersion of 0.057 ps/nm^2/km. All dispersive effects were always fully recovered at the receiver side. Fiber loss was recovered by noiseless optical amplifiers span-by-span. We simulated the link with MATLAB by applying the SSFM to (1). The transmitted sequence length was set longer than the maximum walk-off length over the whole link between the two border channels of the WDM comb, with a minimum value of 4096 symbols. Each symbol was discretized with enough samples to correctly reproduce at least the bandwidth enlargement of first-order FWM without aliasing. A more detailed explanation of the choice of these two parameters is discussed in Appendix B. For efficient FFTs, both parameters have been rounded off to the closest larger integer with factorization containing only powers of 2, 3, 5. The receiver detected the central channel of the comb at $\lambda = 1550$ nm. It was optimized for linear transmission, hence based on a cascade of a matched filter followed by a one tap least squares butterfly equalizer able to recover the average polarization/phase mismatch.[2]

Since a closed form solution of the NLSE is unavailable, we define the SSFM error variance σ^2_{SSFM} at the end of the link as:

$$\sigma^2_{\mathrm{SSFM}} \triangleq \mathrm{var}\left[\widehat{A} - A_{\mathrm{acc}}\right]$$

with $\widehat{A}$ the current SSFM estimation under investigation and A_{acc} our most accurate SSFM solution. We obtained A_{acc} by running simulations at increasing accuracy until observing saturation of $\widehat{\mathrm{SNR}}$. Saturation was reached when the difference of $\widehat{\mathrm{SNR}}$ between two consecutive runs was less than 0.0005 dB. From A_{acc} we also estimated the unit-power NLI variance a_{NL} (7) from the constellation clouds.[3] The accuracy of the variable step-size rules under analysis was investigated by varying the first step size h_1 over a logarithmic grid, i.e., by reducing h_1 by a factor $\sqrt{2}$ between two consecutive runs.

[2]By increasing the number of taps we did not observe any significant change in the SNR ($<$0.01 dB).

[3]a_{NL} is defined as the variance of $\frac{A_{\mathrm{acc}}e^{-j\varphi} - A_{\mathrm{tx}}}{P\sqrt{P}}$ with A_{tx} the transmitted signal and φ the average phase rotation induced by the link.

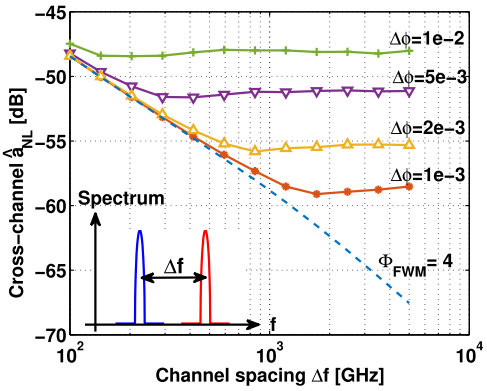

Fig. 2. Estimated cross-channel $\hat{a}_{\mathrm{NL}}$ (7) of a 2-channel simulation at variable channel spacing. Solid lines: Original NLP at various values of $\Delta\phi$; dashed-line: Accurate SSFM with FWM-NLP at $\Phi_{\mathrm{FWM}} = 4$ rad.

IV. Numerical Results

A first evidence of the importance of relating the step size to the signal properties is reported in Fig. 2. The figure shows the estimated unit-power NLI variance $\hat{a}_{\mathrm{NL}}$, affected by numerical noise, for a 2-channel WDM at variable channel spacing. The NLI variance refers to cross-channel interference only, being estimated by removing self-channel distortion from the detected signal. Power was 0 dBm while the link was just one SMF span. In this simplified scenario $\hat{a}_{\mathrm{NL}}$ is expected to be inversely proportional to the channel spacing [23]. However, this is not the case for the original NLP (solid curves) which saturates after a given channel spacing, depending on the value $\Delta\phi$. This is a numerical artifact that can be removed by accounting for the signal bandwidth in the step-size selection, e.g., by starting NLP with our FWM-aware first step choice, as we did for the dashed line in Fig. 2 with $\Phi_{\mathrm{FWM}} = 4$ rad.

We proceed now to show the accuracy dependence on signal and fiber parameters of fully loaded WDM signals.

A. Power Dependence of the SSFM Error

We first checked the dependence of the symmetric SSFM accuracy with the signal power. We compared the nonlinear phase (9) and the constant local error (10) step-updating rules, started with either their corresponding original first step-size choices (11)–(12), or with our FWM-aware choice (13) based on fixing the maximum FWM phase Φ_{FWM} in the first step.

The SSFM accuracy, expressed in terms of the ratio $a_{\mathrm{SSFM}}/a_{\mathrm{NL}}$ (see (7) where $\sigma^2_{\mathrm{SSFM}}/\sigma^2_{\mathrm{NLI}} \equiv a_{\mathrm{SSFM}}/a_{\mathrm{NL}}$) is reported in Fig. 3 for a 20 × 100 km single mode fiber (SMF) link ($D = 17$ ps/nm/km) versus channel power. Small values of $a_{\mathrm{SSFM}}/a_{\mathrm{NL}}$ indicate an accurate simulation, as visible in the graph by looking at the right vertical axis reporting the SNR relative error, which is related to $a_{\mathrm{SSFM}}/a_{\mathrm{NL}}$ by (6)–(7). Although the SNR error is the key performance estimator, it may be more useful to evaluate $a_{\mathrm{SSFM}}/a_{\mathrm{NL}}$ which is more sensitive to small variations of SSFM noise. Please note that at $P = 0$ dBm our most accurate estimation yielded $a_{\mathrm{NL}} = 9.3 \cdot 10^{-3}$ mW^{-2}.

We set the first step per span h_1 equal to 20, 40 or 400 m at $P = 0$ dBm (Fig. 3(a), (b) and (c), respectively). For different powers we either chose h_1 according to the original indications of the NLP, eq. (11), and the CLE, eq (12), respectively, or by keeping it constant as suggested by our FWM-aware proposal (13) (FWM-NLP/FWM-CLE). From the figures we note that our choice (13) grants an almost constant error whatever the power, thus conforming to our expectations, as discussed in Section II and Fig. 1. The original NLP and the CLE methods instead shorten the first step at increasing power, thereby excessively increasing the accuracy at large powers, thus resulting in an increasing waste of computational resources.

For big first step-size (Fig. 3c) even for FWM-NLP/FWM-CLE the accuracy becomes non-flat at high power, although resulting in decreasing SNR error, thus keeping the estimations conservative.

B. Dispersion and Bandwidth Dependence of SSFM Error

To study the dependence of the accuracy on dispersion and bandwidth, we analyzed the scaling of the ratio $a_{\mathrm{SSFM}}/a_{\mathrm{NL}}$ at variable Φ_{FWM} in a 101 channel WDM signal at fixed launch power per channel $P = 0$ dBm. We first report the SSFM relative error versus fiber dispersion in Fig. 4(a), for the symmetric SSFM and the two step-size updating rules considered in the previous section started with our FWM-aware first step choice (13), namely FWM-NLP and FWM-CLE. Each curve refers to a different value of fiber dispersion. Note that increasing Φ_{FWM} means increasing the step size, i.e., decreasing the accuracy of the simulation. Both step-size updating rules show overlapping curves at the various dispersions. Hence, fixing a value of Φ_{FWM} grants the same accuracy at all considered dispersions. Our FWM-aware choice on the first step (13) is thus able to track the accuracy variations due to fiber dispersion. This is not the case for the original NLP (11), reported in Fig. 4(b), which is unaware of the fiber dispersion. It is worth noting that for the 101 channel WDM system at a typical channel launch power of 0 dBm an SNR error smaller than 0.01 dB calls for a $\Delta\phi < 2 \cdot 10^{-4}$ rad at $D = 17$ ps/nm/km, a value well below the typical values usually found in the literature.

The dependence of the accuracy on the signal bandwidth is instead reported in Fig. 5 for the symmetric SSFM. We plotted the ratio $a_{\mathrm{SSFM}}/a_{\mathrm{NL}}$ versus the maximum FWM phase shift Φ_{FWM} in the first step for both the FWM-NLP and FWM-CLE. Each curve in the plots refers to a WDM signal with a different number of channels, starting from a single-channel transmission and up to 101 channels, i.e., a full C-band WDM system. All the curves with more than 3 channels overlap, which highlights the insensitivity of our choice (13) based on Φ_{FWM} to the total system bandwidth. As we can see from Fig. 5, a reasonable target SNR error of 0.01 dB can be reached with Φ_{FWM} equal to $\simeq 20$ rad and $\simeq 4$ rad for the FWM-CLE and the FWM-NLP, respectively.

C. Distance Dependence of SSFM Error

The dependence of SSFM accuracy on propagation distance is shown in Fig. 6. We plotted the variations of $a_{\mathrm{SSFM}}/a_{\mathrm{NL}}$ versus the number of spans at a fixed value of FWM phase shift in the first step, chosen equal to $\Phi_{\mathrm{FWM}} = 20$ rad, which yields a practical value of accuracy for the FWM-CLE as reported in the previous section. We observe that $a_{\mathrm{SSFM}}/a_{\mathrm{NL}}$ in Fig. 6

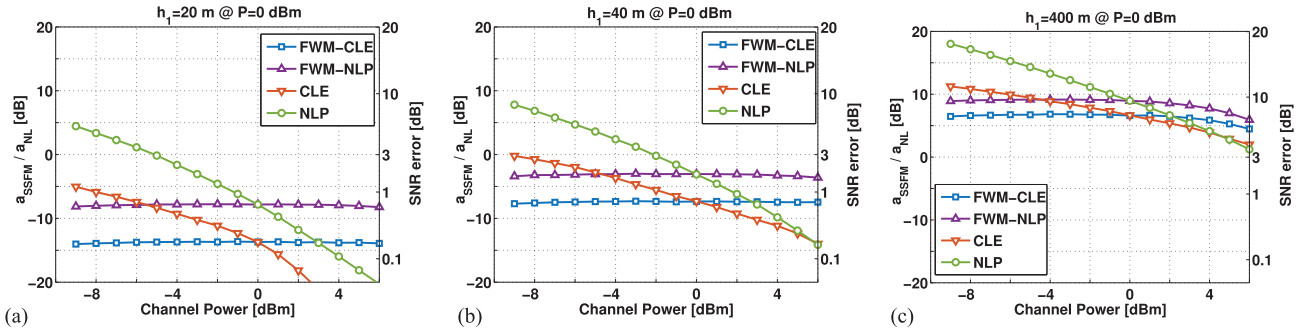

Fig. 3. SSFM accuracy $a_{\mathrm{SSFM}}/a_{\mathrm{NL}}$ vs channel power. The right vertical axis also reports the corresponding SNR relative error. We compare the original nonlinear phase criterion (NLP, eqs. (9), (11)) and the original constant local error method (CLE, eqs. (10), (12)) with our FWM-aware extensions FWM-CLE and FWM-NLP. The first step was set at $P = 0$ dBm to (a) $h_1 = 20$ m, (b) $h_1 = 40$ m and (c) $h_1 = 400$ m and scaled by varying signal power according to the method under analysis. 27 channels WDM signal, 20×100 km SMF link. SSFM with symmetric step.

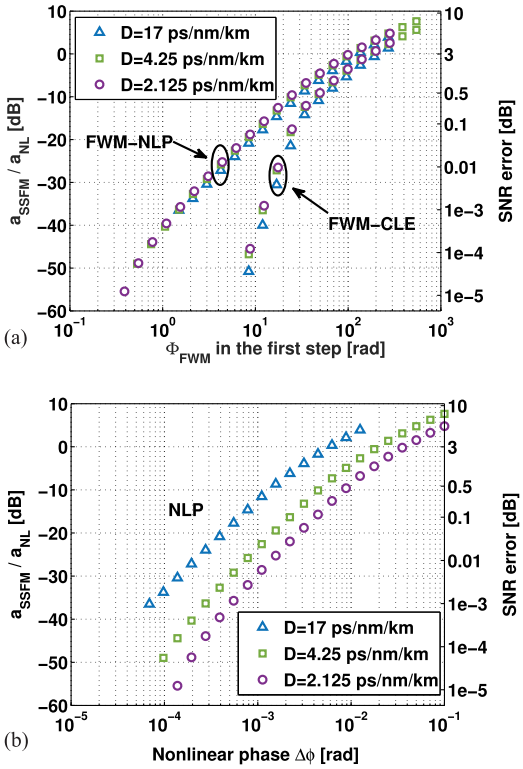

Fig. 4. (a) $a_{\mathrm{SSFM}}/a_{\mathrm{NL}}$ as a function of Φ_{FWM} in the first step. (b) Same as plot (a) but with only the NLP started with its original criterion (11) based on $\Delta\phi$. 101 channel WDM signal (bandwidth of 5 THz). 20×100 km link with variable dispersion. Symmetric SSFM. The corresponding SNR error is shown in the right vertical axis.

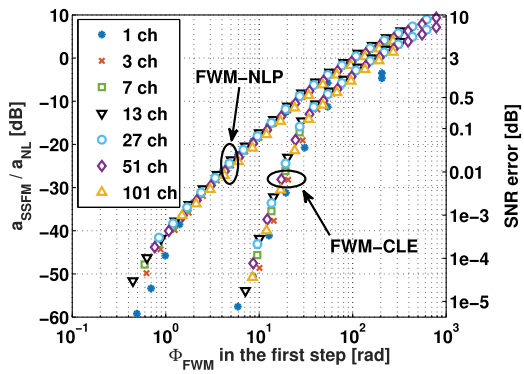

Fig. 5. $a_{\mathrm{SSFM}}/a_{\mathrm{NL}}$ as a function of Φ_{FWM} in the first step for the two different step-updating rules indicated in the graph. Variable number of WDM channels from 1 to 101 (bandwidth of 5 THz). 20×100 km SMF link. Symmetric SSFM. The right axis shows the corresponding SNR error.

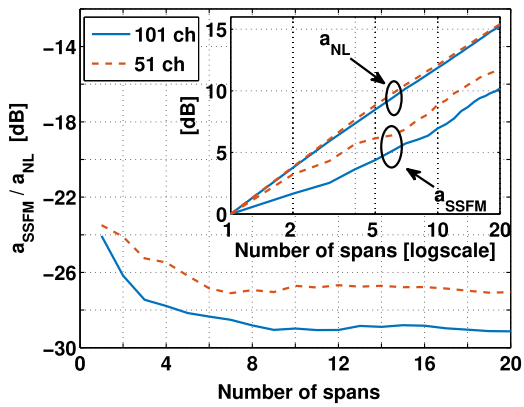

Fig. 6. $a_{\mathrm{NL}}/a_{\mathrm{SSFM}}$ versus number of spans ($\times$ 100 km) at fixed $\Phi_{\mathrm{FWM}} =$ 20 rad. 101 and 51 channel WDM over SMF. Symmetric SSFM with FWM-CLE. Inset: accumulation of a_{NL} and a_{SSFM} along the number of spans. The curves have been normalized to their value at 1 span for an easy comparison.

decreases for increasing number of spans at all bandwidths under investigation, reaching saturation after roughly ten spans. The one span case is thus a worst case for accuracy. The reason for such a decrease is that a_{NL} grows faster with distance with respect to a_{SSFM}, as shown in the inset of Fig. 6. Here we plot separately the accumulation of a_{NL} and a_{SSFM} along the spans for 101 and 51 channel signals. The reason of such a faster-than-linear growth of a_{NL} with distance [21], [22] is related to either the spatial-correlation of NLI [20] and to the impact of signal higher-order statistics in the first spans [19]. On the other hand, we found that a_{SSFM} approaches asymptotically a linear growth for both shown bandwidths. This observation suggests that the SSFM error accumulates approximately incoherently along the distance, a point that we will explore in more detail in the next Section. Even if not reported here to not overcrowd the figure, similar results have been found for all the other considered bandwidths.

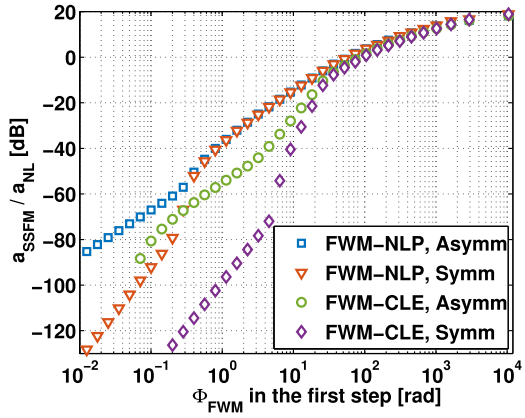

Fig. 7. $a_{\mathrm{SSFM}}/a_{\mathrm{NL}}$ vs Φ_{FWM} in the first step for a 7 channels WDM signal over a single SMF span. FWM-NLP and FWM-CLE with asymmetric and symmetric SSFM.

V. Computational Analysis

According to the Baker-Hausdorff formula, the asymmetric and symmetric SSFM error scales locally with $\mathcal{O}(h^2)$ and $\mathcal{O}(h^3)$, respectively, with h the step length. Common wisdom is that the corresponding global error with constant step-size scales respectively with $\mathcal{O}(h)$ and $\mathcal{O}(h^2)$ [4], [5], [8], similarly to what happens in approximating the integral of a function with the left-point or mid-point rectangle rule. This observation is motivated by the similarities between SSFM and numerical integration, as shown in Section II-A.

In the framework of numerical integration, the global truncation error of the composite left/mid-point rule applied to the integral $\int_0^z f(\xi)\mathrm{d}\xi$ is [24]:

$$e_{\mathrm{G}} = \begin{cases} \sum_{k=1}^{N} \frac{1}{2} h^2 f'(\xi_k) & \text{Asymm. step} \\ \sum_{k=1}^{N} \frac{1}{24} h^3 f''(\xi_k) & \text{Symm. step} \end{cases} \tag{14}$$

where f' and f'' indicate the first and second derivative of the integrand function, respectively. ξ_k is an unknown coordinate inside the kth step, thus $f'(\xi_k)$ and $f''(\xi_k)$ are random processes. In the limit of $h \to 0$, hence $N \to \infty$, the approximation $\sum_k f^{(n)}(\xi_k)h \sim \int f^{(n)}(\xi)\mathrm{d}\xi$, whose result is independent of h, is used to prove the mentioned scaling properties of local and global error [24]. The variance of e_{G} thus scales with $\mathcal{O}(h^2)$ and $\mathcal{O}(h^4)$ for the left and mid-point rule, respectively.

However, it is worth noting that for increasing step-size such an approximation breaks down. In this scenario, the function f is likely to experience many fluctuations within a step, hence the local errors of both the left and mid-point rule are expected to be independent step-by-step. Under ergodic assumptions, they are also identically distributed step-by-step. This way, the numerical integration is more similar to Monte Carlo integration, where the global error variance scales with the inverse of the number of steps, i.e., linearly with the step length h. It is worth noting that such an observation corresponds to having in (14) $hf'(\xi_k)$ and $h^2 f''(\xi_k)$ independent and identically distributed random processes in k.

Such a reasoning holds even for SSFM, as confirmed by Fig. 7, which shows the ratio $a_{\mathrm{SSFM}}/a_{\mathrm{NL}}$ for a 7 channel WDM signal

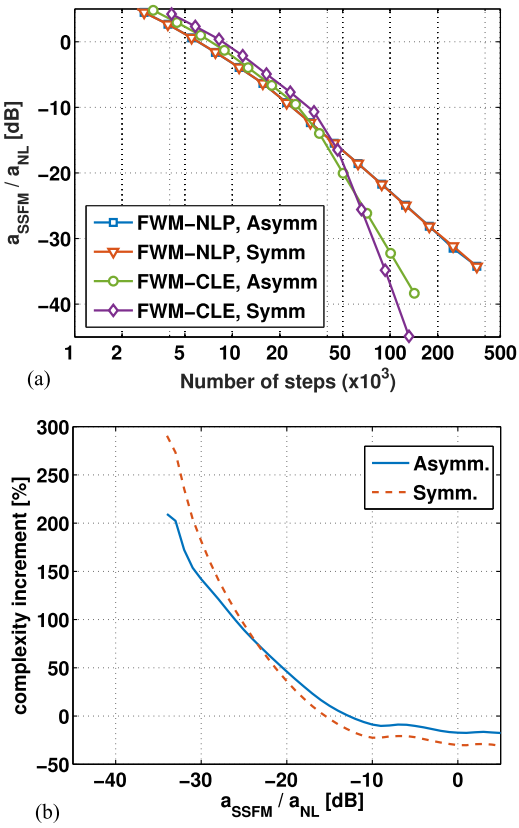

Fig. 8. (a) $a_{\mathrm{SSFM}}/a_{\mathrm{NL}}$ vs number of steps for a 101 channels over a single SMF span and (b) corresponding complexity increment of FWM-NLP with respect to FWM-CLE for asymmetric and symmetric SSFM.

at $P = 0$ dBm over a single SMF span versus Φ_{FWM} in the first step. We chose such a small bandwidth to push the simulations up to very high accuracy in a reasonable amount of time. Here the step size is adaptive with different algorithms, hence we focused on the scaling properties with respect to the first step h_1. Instead of h_1 we report on the x-axis Φ_{FWM} according to (13) which is our target parameter for setting up a SSFM simulation as shown in the previous sections. It is worth noting that the scaling properties predicted by the Baker-Hausdorff formula appear only at $h_1 \ll 1$, i.e., at very small SNR errors usually not of interest, while for coarse steps all the methods converge to the Monte Carlo integration scaling described above. The Monte Carlo region is indeed of particular interest in coarse approximations of SSFM, such as for digital back-propagation techniques for nonlinearity mitigation [25].

In order to compare how such error scaling rules affect the computational effort, we plotted in Fig. 8 a the target $a_{\mathrm{SSFM}}/a_{\mathrm{NL}}$ versus the number of steps for both the FWM-NLP and the FWM-CLE either with asymmetric and symmetric SSFM. The signal here was composed of 101 channels, i.e., the whole C-band. The symmetric SSFM was implemented by combining the linear operators of two consecutive steps as in [3] to have a complexity comparable with that of the asymmetric SSFM. The first observation is that, with the FWM-NLP, asymmetric and symmetric SSFM curves overlap, thus they perform identically at practical accuracy. Moreover, the CLE step-updating rule, which was derived in the region for $h \ll 1$, is not optimal anymore. With coarse steps, we found more efficient the

FWM-NLP as depicted in Fig. 8(b) for the same 101 channel signal. Here we plot the percentage increment of complexity by using the FWM-NLP with respect to the FWM-CLE versus the target $a_{\text{SSFM}}/a_{\text{NL}}$. The increment is defined as $\frac{N_{\text{NLP}}-N_{\text{CLE}}}{N_{\text{CLE}}}$, with N_{NLP} and N_{CLE} the number of steps yielding a given accuracy for the two above-mentioned rules, respectively. At small values of $a_{\text{SSFM}}/a_{\text{NL}}$ the FWM-CLE is more and more efficient, both with symmetric and asymmetric SSFM, while for higher values of $a_{\text{SSFM}}/a_{\text{NL}}$ the saturation of the curves on a negative percentage indicates a complexity reduction by using the FWM-NLP. Even if not reported here, similar results have been found for all the bandwidths under analysis.

VI. Conclusion

We investigated the accuracy of SSFM in the framework of the perturbative solution of the Manakov equation, thus treating the SSFM error as a distributed additive interference. We pushed the signal bandwidth up to 5 THz, i.e., the whole C-band. With our new FWM-aware suggested choice of the initial step size, eq. (13), we showed that the numerical relative error on the SNR at the receiver side is signal-power independent, with a variance scaling with the square of the bandwidth. This behavior is in contrast with the widely used nonlinear phase criterion for step size setup which is power-dependent and unaware of the signal bandwidth, and with the constant local error criterion, which is bandwidth-aware but still power-dependent. In particular, the nonlinear phase criterion showed to be reliable in our 5 THz setup at 0 dBm only for a maximum nonlinear phase per step smaller than $2 \cdot 10^{-4}$ rad, a value usually smaller than what is used in the literature. Our initial step choice proposal (13) based on bounding the amount of FWM phase shift inside the first step grants an almost-constant accuracy of the simulation at variable signal power, fiber parameters and signal bandwidth. This is extremely useful as a plug-and-play universal SSFM setup in today's ultra-wideband systems simulations with guaranteed SNR accuracy.

Moreover, we compared in terms of complexity two popular step-updating rules, i.e., the one implicit in the nonlinear phase criterion and another one based on keeping a constant local error in the step, for a wide range of SNR accuracy. We showed that the assumptions at the basis of the constant local error rule hold only for very accurate simulations, i.e., for very small steps. On the contrary, for coarse steps we found more efficient the step-updating rule given by the nonlinear phase criterion, which can thus find application in coarse SSFM implementations such as digital back-propagation. Finally, we gave general indications on how to set up a correct SSFM simulation in terms of sequence length and signal discretization.

Appendix A
SSFM as Numerical Integration

In this Appendix, we derive the asymmetric and symmetric step SSFM from the integral form of the NLSE. We start from the NLSE:

$$\frac{\partial A}{\partial z} = (\mathcal{L} + \mathcal{N})A$$

where $\mathcal{L}$ and $\mathcal{N}$ are defined in (2). In the reference system tracking linear effects, i.e., $A(z,t) \triangleq e^{\mathcal{L}z}U(z,t)$, we have:

$$\frac{\partial U}{\partial z} = e^{-\mathcal{L}z}\mathcal{N}\left(e^{\mathcal{L}z}U\right)$$

where $e^{\mathcal{L}z}$ can be read as a shorthand notation for the linear convolution with linear effects. In integral form the differential equation takes the expression:

$$U(z,t) = U(0,t) + \int_0^z e^{-\mathcal{L}\xi}\mathcal{N}\left(e^{\mathcal{L}\xi}U(\xi,t)\right)\mathrm{d}\xi.$$

The key idea of SSFM is to substitute $e^{\mathcal{L}\xi}$ with $e^{\mathcal{L}\xi_0}$, with ξ_0 a fixed coordinate within the step $[0,z]$, such that we get:

$$U(z,t) \simeq U(0,t) + e^{-\mathcal{L}\xi_0}\int_0^z \mathcal{N}\left(e^{\mathcal{L}\xi_0}U(\xi,t)\right)\mathrm{d}\xi\,.$$

By the change of variable $E(z,t) \triangleq e^{\mathcal{L}\xi_0}U(z,t)$ we have

$$E(z,t) = E(0,t) + \int_0^z \mathcal{N}\left(E(\xi,t)\right)\mathrm{d}\xi$$

whose closed form solution is $E(z,t) = e^{\int_0^z \mathcal{N}\mathrm{d}\xi}E(0,t)$. Since $E(z,t) = e^{\mathcal{L}(\xi_0 - z)}A(z,t)$, in the original reference system we have:

$$A(z,t) \simeq e^{\mathcal{L}(z-\xi_0)}e^{\int_0^z \mathcal{N}\mathrm{d}\xi}e^{\mathcal{L}\xi_0}A(0,t)\ .$$

Finally, by substituting $\xi_0 = 0$ and $\xi_0 = \frac{z}{2}$ we obtain the asymmetric and symmetric step SSFM:

$$A(z,t) \simeq \begin{cases} e^{\mathcal{L}z}e^{\int_0^z \mathcal{N}\mathrm{d}\xi}A(0,t) & \text{asymm-step} \\ e^{\mathcal{L}\frac{z}{2}}e^{\int_0^z \mathcal{N}\mathrm{d}\xi}e^{\mathcal{L}\frac{z}{2}}A(0,t) & \text{symm-step}\,. \end{cases}$$

Appendix B
Signal Discretization

In this Appendix we provide general rules to set up an accurate SSFM simulation.

A. Numerical Bandwidth

Signals have to be sampled in a numerical simulation. The correct number of samples N_{t} per symbol to avoid frequency aliasing on a digital signal is given by the Nyquist-Shannon theorem and must satisfy:

$$B_{\text{Nt}} \triangleq N_{\text{t}}R \geq \kappa \cdot B_{\text{WDM}}$$

where R is the channel symbol rate and B_{WDM} the bandwidth of the signal entering the fiber. $\kappa \geq 1$ is an expansion factor to account for the signal bandwidth enlargement due to FWM. Such a factor is set by the user depending on how much FWM one wants to correctly reproduce. For example, to avoid aliasing on the first-order FWM, the simulation bandwidth should be set to $B_{\text{Nt}} \geq 3B_{\text{WDM}}$ as sketched in Fig. 9. By defining FWM_{out}, FWM_{in} and FWM_{CUT} the first order FWM falling outside the WDM bandwidth B_{WDM}, inside the WDM bandwidth and inside the bandwidth of the channel under test (CUT), Table I reports the minimum value of B_{Nt} needed to avoid aliasing on each FWM component.

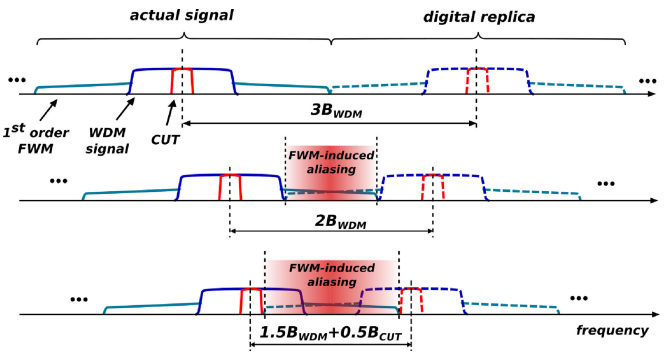

Fig. 9. Sketch of the FWM-aliasing problem due to discretization. The first-order FWM does not induce aliasing for a simulation bandwidth $B_{\text{Nt}} \geq 3B_{\text{WDM}}$. B_{CUT} is the bandwidth of the channel under test.

TABLE I
NUMERICAL BANDWIDTH B_{Nt} SETUP TO CORRECTLY REPRODUCE FIRST ORDER FWM

B_{Nt}	FWM_{out}	FWM_{in}	FWM_{CUT}
$\geq 3B_{\text{WDM}}$	✓	✓	✓
$\geq 2B_{\text{WDM}}$		✓	✓
$\geq \frac{3}{2}B_{\text{WDM}} + \frac{1}{2}B_{\text{CUT}}$			✓

B. Sequence Length

While propagating a WDM signal along an optical link, each channel experiences a specific group delay. Since digital sequences are intrinsically periodic due to discrete Fourier transform operations, if the walk-off is longer than the sequence length temporal-aliasing occurs, which can lead to artificial correlations in circular convolutions. To completely avoid this numerical artifact the sequence length N_{seq} should be longer than the maximum walk-off between the side frequencies of the WDM signal, i.e.:

$$N_{\text{seq}} = |D_{\text{cum}}|\, B_{\text{WDM}} \frac{\lambda^2}{c} R \cdot 10^{-3} \quad [\text{symbols}]$$

where B_{WDM} [GHz] is the WDM bandwidth, R [Gbaud] the channel symbol rate, λ [nm] the central wavelength of the WDM comb, c [m/s] the speed of light, D_{cum} [ps/nm] the peak-to-peak accumulated dispersion along the link. In particular, for dispersion uncompensated links D_{cum} is the dispersion accumulated from input to output.

As a reference, the 101-channel curves of Fig. 5 ($B_{\text{WDM}} = 5$ THz) call for $N_{\text{seq}} > 66709$ symbols.

ACKNOWLEDGMENT

The authors would like to thank P. Ramantanis and M. Lonardi for valuable comments and suggestions. This research benefits from the high performance computing facility of the University of Parma, Italy.

REFERENCES

[1] G. P. Agrawal, *Nonlinear Fiber Optics*, 5th ed. New York, NY, USA: Academic, 2013.
[2] G. Strang, "On the construction and comparison of difference schemes," *SIAM J. Numer. Anal.*, vol. 5, no. 3, pp. 506–517, 1968.
[3] J. Shao, X. Liang, and S. Kumar, "Comparison of split-step Fourier schemes for simulating fiber optic communication systems," *IEEE Photon. J.*, vol. 6, no. 4, pp. 1–15, Aug. 2014.
[4] O. V. Sinkin, R. Holzlöhner, J. Zweck, and C. R. Menyuk, "Optimization of the split-step Fourier method in modeling optical fiber communications systems," *J. Lightw. Technol.*, vol. 21, no. 1, pp. 1–27, Jan. 2003.
[5] G. M. Muslu and H. A. Erbay, "Higher-order split-step Fourier schemes for the generalized nonlinear Schrödinger equation," *Math. Comput. Simul.*, vol. 67, no. 6, pp. 581–595, Jan. 2005.
[6] G. Bosco, A. Carena, V. Curri, R. Gaudino, P. Poggiolini, and S. Benedetto, "Suppression of spurious tones induced by the split-step method in fiber systems simulation," *IEEE Photon. Technol. Lett.*, vol. 12, no. 5, pp. 489–491, May 2000.
[7] Q. Zhang and M. I. Hayee, "An SSF scheme to achieve comparable global simulation accuracy in WDM systems," *IEEE Photon. Technol. Lett.*, vol. 17, no. 9, pp. 1869–1871, Sep. 2005.
[8] Q. Zhang and M. I. Hayee, "Symmetrized split-step Fourier scheme to control global simulation accuracy in fiber-optic communication systems," *J. Lightw. Technol.*, vol. 26, no. 2, pp. 302–315, Jan. 2008.
[9] C. Francia, "Constant step-size analysis in numerical simulation for correct four-wave-mixing power evaluation in optical fiber transmission systems%," *IEEE Photon. Technol. Lett.*, vol. 11, no. 1, pp. 69–71, Jan. 1999.
[10] A. Ghazisaeidi *et al.*, "Advanced C + L-band transoceanic transmission systems based on probabilistically shaped PDM-64QAM," *J. Lightw. Technol.*, vol. 35, no. 7, pp. 1291–1299, Apr. 2017.
[11] J.-X. Cai *et al.*, "51.5 Tb/s capacity over 17,107 km in C + L bandwidth using single mode fibers and nonlinearity compensation,"*J. Lightw. Technol.*, vol. 36, no. 11, pp. 2135–2141, Jun. 2018.
[12] S. Musetti, P. Serena, and A. Bononi, "Constant SNR-Error step-size selection rule for numerical simulation of optical transmissions," in *Proc. Eur. Conf. Opt. Commun.*, Gothenburg, Sweden, 2017, Paper P2.SC6.24.
[13] P. K. A. Wai and C. R. Menyuk, "Polarization mode dispersion, decorrelation, and diffusion in optical fibers with randomly varying birefringence, *J. Lightw. Technol.*, vol. 14, no. 2, pp. 148–157, Feb. 1996.
[14] D. Marcuse, C. R. Menyuk, and P. K. A. Wai, "Application of the Manakov-PMD equation to studies of signal propagation in optical fibers with randomly varying birefringence," *J. Lightw. Technol.,* vol. 15, no. 9, pp. 1735–1746, Sep. 1997.
[15] M. Cantono, D. Pilori, A. Ferrari, A. Carena, and V. Curri, "Observing the interaction of PMD with generation of NLI in uncompensated amplified optical links," in *OFC, Proc.* San Diego, CA, USA, 2018, Paper W1G.4.
[16] A. Vannucci, P. Serena, and A. Bononi, "The RP method: A new tool for the iterative solution of the nonlinear Schrödinger equation," *J. Lightw. Technol.*, vol. 20, no. 7, pp. 1102–1112, Jul. 2002.
[17] A. Iserles and S. P. Nørsett, "Efficient quadrature of highly oscillatory integrals using derivatives," *Proc. R. Soc. A Math. Phys. Eng. Sci.*, vol. 461, no. 2057, pp. 1383–1399, May 2005.
[18] P. Poggiolini, G. Bosco, A. Carena, V. Curri, Y. Jiang, and F. Forghieri, "The GN-model of fiber nonlinear propagation and its applications," *J. Lightw. Technol.*, vol. 32, no. 4, pp. 694–721, Feb. 2014.
[19] A. Mecozzi and R. Essiambre, "Nonlinear Shannon limit in pseudolinear coherent systems," *J. Lightw. Technol.*, vol. 30, no. 12, pp. 2011–2024, Jun. 2012.
[20] P. Serena and A. Bononi, "An alternative approach to the Gaussian noise model and its system implications," *J. Lightw. Technol.*, vol. 31, no. 21, pp. 3489–3499, Nov. 2013.
[21] A. Carena, V. Curri, G. Bosco, P. Poggiolini, and F. Forghieri, "Modeling of the impact of nonlinear propagation effects in uncompensated optical coherent transmission links," *J. Lightw. Technol.,* vol. 30, no. 10, pp. 1524–1539, May 2012.
[22] A. Bononi, N. Rossi, and P. Serena, "On the nonlinear threshold versus distance in long-haul highly-dispersive coherent systems," *Opt. Express*, vol. 20, no. 26, pp. B204–B216, Dec. 2012.
[23] O. Rival and K. Mheidly, "Accumulation rate of inter and intra-channel nonlinear distortions in uncompensated 100G PDM-QPSK systems," in *Proc. OFC*, Los Angeles, CA, USA, 2012, Paper JW2A.52.
[24] J. H. Mathews and K. D. Fink, *Numerical Methods Using MATLAB*. Englewood Cliffs, NJ, USA: Prentice Hall, 1999.
[25] E. Ip and J. M. Kahn, "Compensation of dispersion and nonlinear impairments using digital backpropagation," *J. Lightw. Technol.*, vol. 26, no. 20, pp 3416–3425, Oct. 2008.

Authors' biographies not available at the time of publication.